BIT Numer Math (2016) 56:1479–1496
DOI 10.1007/s10543-016-0611-3

Entropy solutions of the compressible Euler equations

Magnus Svärd[1]

Received: 11 September 2015 / Accepted: 22 February 2016 / Published online: 2 March 2016

Abstract We consider the three-dimensional Euler equations of gas dynamics on a bounded periodic domain and a bounded time interval. We prove that Lax–Friedrichs scheme can be used to produce a sequence of solutions with ever finer resolution for any appropriately bounded (but not necessarily small) initial data. Furthermore, with some technical assumptions, e.g. that the density remains strictly positive in the sequence of solutions at hand, a subsequence converges to an entropy solution. We provide numerical evidence for these results by computing a sensitive Kelvin–Helmholtz problem.

Keywords Euler equations · Weak solutions · Entropy solutions · Convergence · Lax–Friedrichs scheme

Mathematics Subject Classification 35L65 · 65M12 · 76N10

1 Introduction

In three space dimensions, the compressible Euler equations on conservative form are,

$$\mathbf{u}_t + \mathbf{f}^1_x + \mathbf{f}^2_y + \mathbf{f}^3_z = 0 \tag{1.1}$$

Communicated by Jan Nordström.

✉ Magnus Svärd
Magnus.Svard@uib.no

[1] Department of Mathematics, University of Bergen, Postbox 7800, 5020 Bergen, Norway

where

$$\begin{aligned}\mathbf{f}^1 &= (\rho u,\, \rho u^2 + p,\, \rho uv,\, \rho uw,\, u(E+p))^T,\\ \mathbf{f}^2 &= (\rho v,\, \rho vu,\, \rho v^2 + p,\, \rho vw,\, v(E+p))^T,\\ \mathbf{f}^3 &= (\rho w,\, \rho wu,\, \rho wv,\, \rho w^2 + p,\, w(E+p))^T,\\ \mathbf{u} &= (\rho,\, \rho \mathbf{v}^T,\, E)^T \quad \text{conservative variables.}\end{aligned} \tag{1.2}$$

$\mathbf{v}$ denotes the velocity vector with components (u, v, w); ρ is the density, p the pressure, E the total energy, e the specific internal energy and, T the temperature. c_p and c_v denote the specific heats at constant pressure or volume. Furthermore, $E = \frac{1}{2}\rho|\mathbf{v}|^2 + \rho e$, $e = c_v T$, $\rho e = \frac{p}{\gamma - 1}$ and $\gamma = c_p/c_v$. (For air, $\gamma = 7/5$ but generally $1 < \gamma < 5/3$.) The thermodynamic variables are related through the ideal gas law, $p = \rho RT$ where R is the gas constant.

In this paper, we consider the Euler equations (1.1) on the domain $\mathscr{Q} = [0, \mathscr{T}] \times \Omega$, where $\mathscr{T}$ is an arbitrary but finite time and $\Omega = [0, 1]^3$ is the unit cube. We assume periodicity in all three space dimensions.

Assumption 1.1 Assume that the initial data are provided in the following spaces:

$$\mathbf{u}(0, \mathbf{x}) \in (L^2(\Omega))^5, \quad T(0, \mathbf{x}) \in L^2(\Omega), \quad \mathbf{v}(0, \mathbf{x}) \in (L^2(\Omega))^3, \quad \rho(0, \mathbf{x}), T(0, \mathbf{x}) > 0.$$

For initial data with small total variation, existence and uniqueness have been proven in [1] for the 1-D problem. However, to date there are no global well-posedness results for the system of Euler equations in 3-D. The goal of this work is to address the question of existence of so-called (weak) entropy solutions.

1.1 Definitions

It is well-known that the Euler equations may develop discontinuities in finite time. Therefore its solutions are usually interpreted in a weak sense.

A solution $\mathbf{u}$ is a *weak solution*, if it satisfies the equations in a distributional sense. That is, if $\mathbf{u}$ satisfies

$$\int_0^T \int_\Omega \left((\phi_t)\mathbf{u} + (\phi_x)\mathbf{f}^1 + (\phi_y)\mathbf{f}^2 + \phi_z \mathbf{f}^3 \right) d\mathbf{x}\, dt + \int_\Omega \phi(\mathbf{x}, 0)\mathbf{u}(0, \mathbf{x})\, d\mathbf{x} = 0 \tag{1.3}$$

for all non-negative test functions $\phi \in \mathscr{D}(\mathscr{Q})$ (these functions are periodic since Ω is periodic). Weak solutions are generally not unique and conservation laws, such as (1.1), are supplemented with an entropy condition. To define the entropy condition, we need the following definition.

Definition 1.1 Let d be the number of space dimensions. An *entropy pair*, is a pair of functions $(U, \mathbb{F})$ with $U : \mathbb{R}^5 \to \mathbb{R}$, $\mathbb{F} : \mathbb{R}^5 \to \mathbb{R}^d$ where U is convex and $\mathbb{F}' = U'\mathbf{f}'$.

Here, we consider three space dimensions, i.e., $d = 3$ and $\mathbb{F} = (F^1, F^2, F^3)$. Furthermore, $\mathbf{q}^T = U_{\mathbf{u}}$ are the *entropy variables*. We denote the entropy potential as $\Psi^i = \langle \mathbf{q}, \mathbf{f}^i(\mathbf{u}(\mathbf{q}))\rangle - F^i(\mathbf{u}(\mathbf{q}))$, $i = 1, 2, 3$. A vanishing viscosity solution of a conservation law, results in the following inequality for the entropy pair.

$$U_t + \nabla \mathbb{F} \leq 0 \tag{1.4}$$

Since solutions of conservation laws are often assumed to be a vanishing viscosity limits of a viscous equation, (1.4) is often used as an entropy condition or admissibility criterion.

Definition 1.2 A weak solution $\mathbf{u}$ of (1.1) is an *entropy solution*, if (1.4) is satisfied in a distributional sense for *all* entropy pairs.

For the Euler equations, it is not clear if this entropy condition will single out a unique solution. As mentioned above, the entropy inequality is satisfied for vanishing viscosity solutions but other entropy conditions have been proposed. We refer to [6] for a discussion on entropy conditions for the Euler equations.

Let $S = \ln(\frac{p}{\rho^\gamma})$ be the specific entropy. Then the entropy pairs for the Euler equations are given by

$$\begin{aligned} U &= -\rho h(S) \\ F^1 &= -\rho u h(S), \\ F^2 &= -\rho v h(S), \\ F^3 &= -\rho w h(S), \\ \frac{h''(S)}{h'(S)} &< \frac{1}{\gamma} \qquad \text{(See [5].)} \end{aligned}$$

For an entropy U, $U_{\mathbf{uu}}$ is symmetric positive definite. (For the Euler equations this is the case if $\rho, T > 0$.)

Integrating (1.4) over Ω leads to the familiar global entropy *inequality*.

$$\int_\Omega U_t \, d\mathbf{x} \leq 0. \tag{1.5}$$

The inequality (1.5) results in a bound on $U(\mathscr{T})$, which leads to the following result, which is standard. (See [3].)

Proposition 1.1 *Assume that the initial conditions are given as in Assumption 1.1. Furthermore, we assume that* $\rho(\mathbf{x}, t) > 0, T(\mathbf{x}, t) > 0$, $t \in [0, \mathscr{T}], \mathbf{x} \in \Omega$. *Then* entropy solutions $\mathbf{u}$ *of* (1.1), *satisfy*

$$\mathbf{u}(t) \in (L^2(\Omega))^5, \quad p, \rho|\mathbf{v}|^2 \in L^2(\Omega). \tag{1.6}$$

Such estimates are possible to obtain for numerical schemes (so-called entropy stable schemes). However, they are not sufficient to prove convergence to a weak solution. The problem is the non-linear flux function.

Our strategy is the following. We use (essentially) the local Lax–Friedrichs scheme, in a semi-discrete form, and demonstrate that it generates a sequence of solutions up to any finite time on the bounded periodic domain. This part is accomplished with the help of entropy estimates and a proof that the thermodynamic variables remain non-negative to any final time $\mathscr{T}$.

Having established that a sequence of solutions can be generated on ever finer grids, we consider sequences that have no vacuum regions. (We regard this as an *a posteriori* examination since an existing sequence either has this property or not.) For sequences whose density remain bounded away from 0 (and another technical assumption), we prove convergence to a weak entropy solution.

Finally, we present numerical results for a Kelvin–Helmholtz problem that is very sensitive to perturbations. Numerical simulations of this problem were used in [4] as evidence of the *non-existence* of entropy solutions. Contrary to their results, we do see convergence to an entropy solution. This is in accordance with the main conclusion in this paper: If a numerical simulation of Lax–Friedrichs scheme is "well-behaved", then the solution approximates a weak entropy solution.

2 Lax–Friedrichs scheme

We discretize the domain Ω with $N+1$ points in the x, y, z directions. That means $h = 1/N$ and $x_i = ih$, $y_j = jh$, and $z_k = kh$, $i, j, k = 0, \ldots, N$. Let $\mathbf{u}^h_{ijk} = (\rho_{ijk}, m^1_{ijk}, m^2_{ijk}, m^3_{ijk}, E_{ijk})^T$ where the components are the numerical variables corresponding to density, momentum in the x-y-z-direction and total energy. All variables satisfy the same algebraic relations as their continuous counterparts. E.g. $E_{ijk} = \frac{p_{ijk}}{\gamma-1} + \frac{1}{2\rho_{ijk}}((m^1_{ijk})^2 + (m^2_{ijk})^2 + (m^3_{ijk})^2)$. We use u_{ijk}, v_{ijk} and w_{ijk} to denote the velocity components. With a slight abuse of notation, we use D^x_- to denote the operator $D^x_- a_{ijk} = \frac{a_{ijk}-a_{i-1jk}}{h}$ irrespective if a is a scalar or a vector. If it is a vector, the operation is carried out on each component. We define D^y_-, D^z_-, D^x_+, D^y_+, D^z_+ analogously. Furthermore, $D_0 = \frac{1}{2}(D_+ + D_-)$.

The periodic boundary conditions are enforced through the following relations:

$$\mathbf{u}^h_{0jk} = \mathbf{u}_{N+1jk}, \quad \mathbf{u}^h_{i0k} = \mathbf{u}_{iN+1k}, \quad \mathbf{u}^h_{ij0} = \mathbf{u}_{ijN+1}. \tag{2.1}$$

Let

$$\begin{aligned}
\mathbf{g}^1_{ijk} &= (m^1_{ijk}, u_{ijk}m^1_{ijk} + p_{ijk}, u_{ijk}m^2_{ijk}, u_{ijk}m^3_{ijk}, u_{ijk}(E_{ijk} + p_{ijj}))^T, \\
\mathbf{g}^2_{ijk} &= (m^2_{ijk}, v_{ijk}m^1_{ijk}, v_{ijk}m^2_{ijk} + p_{ijk}, v_{ijk}m^3_{ijk}, v_{ijk}(E_{ijk} + p_{ijk}))^T, \\
\mathbf{g}^3_{ijk} &= (m^3_{ijk}, w_{ijk}m^1_{ijk}, w_{ijk}m^2_{ijk}, w_{ijk}m^3_{ijk} + p_{ijk}, w_{ijk}(E_{ijk} + p_{ijk}))^T,
\end{aligned}$$

be the local flux vectors at the grid points. The semi-discrete local Lax–Friedrichs scheme is,

$$(\mathbf{u}^h_{ijk})_t + D^x_- \mathbf{f}^1_{i+1/2jk} + D^y_- \mathbf{f}^2_{ij+1/2k} + D^z_- \mathbf{f}^3_{ijk+1/2} = 0. \tag{2.2}$$

where

$$\begin{aligned}
\mathbf{f}^1_{i+1/2jk} &= \frac{\mathbf{g}^1_{i+1jk} + \mathbf{g}^1_{ijk}}{2} - \frac{\lambda^1_{i+1/2jk}}{2}(\mathbf{u}_{i+1,jk} - \mathbf{u}_{ijk}),\\
\mathbf{f}^2_{ij+1/2k} &= \frac{\mathbf{g}^2_{ij+1k} + \mathbf{g}^2_{ijk}}{2} - \frac{\lambda^2_{ij+1/2k}}{2}(\mathbf{u}_{ij+1k} - \mathbf{u}_{ijk}),\\
\mathbf{f}^3_{ijk+1/2} &= \frac{\mathbf{g}^3_{ijk+1} + \mathbf{g}^3_{ijk}}{2} - \frac{\lambda^3_{ijk+1/2}}{2}(\mathbf{u}_{ijk+1} - \mathbf{u}_{ijk}),
\end{aligned} \tag{2.3}$$

and

$$\begin{aligned}
\lambda^1_{i+1/2jk} &= \max(|u_{i+1jk}| + c_{i+1jk}, |u_{ijk}| + c_{ijk}) + \delta\\
\lambda^2_{ij+1/2k} &= \max(|v_{ij+1k}| + c_{ij+1k}, |v_{ijk}| + c_{ijk}) + \delta\\
\lambda^3_{ijk+1/2} &= \max(|w_{ijk+1}| + c_{ijk+1}, |w_{ijk}| + c_{ijk}) + \delta
\end{aligned} \tag{2.4}$$

where $\delta > 0$ is a constant.

Remark 2.1 With $\delta = 0$ the scheme is the semi-discrete Local Lax–Friedrichs scheme. For technical reasons, we need an (arbitrarily) small extra diffusion δ.

The numerical entropy flux in the x-direction is

$$\mathbf{F}^1_{i+1/2jk} = \frac{1}{2}\langle \mathbf{q}_{i+1jk} + \mathbf{q}_{ijk}, \mathbf{f}^1_{i+1/2jk}\rangle - \frac{1}{2}\left(\Psi^1_{i+1jk} + \Psi^1_{ijk}\right). \tag{2.5}$$

Entropy stability ensures that

$$\langle \mathbf{q}_{i+1jk} - \mathbf{q}_{ijk}, \mathbf{f}^1_{i+1/2jk}\rangle \le \left(\Psi^1_{i+1jk} - \Psi^1_{ijk}\right). \tag{2.6}$$

(Similar relations hold in the other two directions). The key idea with entropy stability is that upon contraction of (2.2) with the entropy variables, $\mathbf{q}_{ijk}$, one obtains,

$$(U_{ijk})_t + \mathbf{q}^T_{ijk}(D^x_- \mathbf{f}^1_{i+1/2jk} + D^y_- \mathbf{f}^2_{ij+1/2k} + D^z_- \mathbf{f}^3_{ijk+1/2}) = 0$$

which can be recast using the entropy stability properties (2.5) and (2.6) as,

$$(U_{ijk})_t + D^x_- \mathbf{F}^1_{i+1/2jk} + D^y_- \mathbf{F}^2_{ij+1/2k} + D^z_- \mathbf{F}^3_{ijk+1/2} \le 0. \tag{2.7}$$

Note that (2.7) is *a local entropy inequality in every point* and corresponds to (1.4). A numerical solution obtained with (2.2) will satisfy the entropy condition (i.e. it is *entropy stable*) for all entropies. (See [9].) Hence, if the discrete solutions converge as the grid is refined, the limit will be an *entropy solution*.

2.1 The discrete entropy estimate

We will use the notation $L^2(\Omega_N)$ to denote the discrete L^2-space. It is equipped with the norm, $\|u^h\|_2^2 = \sum_{ijk=0}^N h^3 u_{ijk}^2$ where u^h denotes the entire vector of (in this case x-velocity) values u_{ijk}. (Other discrete norms are defined with the same analogy.)

We will use the superscript h to distinguish a discrete vector from the corresponding continuous variable. E.g. $\mathbf{u}(x,t)$ is the continuous vector with five components appearing in the Euler equations. $\mathbf{u}_{ijk}$ is the discrete solution vector with five components at x_i, y_j, z_k. $\mathbf{u}^h$ is the vector of all discrete solutions at all points such that $(\mathbf{u}^h)_{ijk} = \mathbf{u}_{ijk}$. The analogous relations hold for all variables, including scalars.

Assumption 2.1 The initial data are projections of the initial data given in Assumption 1.1 onto the grid. That is $\mathbf{u}_{ijk}^0 = \mathbf{u}(0, \mathbf{x}_{ijk})$. Hence, the discrete initial data reside in the equivalent discrete spaces.

Proposition 2.1 *Let the initial data be given as in Assumption 2.1. Assume that* $T^h(t), \rho^h(t) \geq 0$, $t \in [0, \mathscr{T}]$, *then the scheme (2.2) is entropy stable and its solutions satisfy* $\mathbf{u}^h \in C(0, \mathscr{T}; (L^2(\Omega_N))^5)$ *and* $p^h, (\rho(u^2+v^2+w^2))^h \in C(0, \mathscr{T}; L^2(\Omega_N))$.

Proof Multiplying (2.7) by h^3 and summing in (periodic) space, lead to,

$$\sum_{i,j,k=0}^{N} h^3 (U_{ijk})_t \leq 0 \tag{2.8}$$

To obtain an L^2 bound on the variables, we repeat the calculation for the entropy $\bar{U} = U - U(\mathbf{u}_0^h) - U'(\mathbf{u}_0^h)^T(\mathbf{u}^h - \mathbf{u}_0^h)$ where $\mathbf{u}_0^h$ is a constant state. (This is an affine change, which ensures that $\bar{U}$ is also an entropy.) We choose $(\mathbf{u}_0)_{ijk} = (\rho_0, 0, 0, 0, E_0)$, for all i, j, k, where ρ_0 and E_0 are positive constants. This corresponds to a state at rest with constant density, temperature and pressure.

The entropy $\bar{U}$ satisfies the analog estimate (2.8). We can recast this as

$$\frac{1}{2} \sum_{i,j,k=0}^{N} \{h^3 (\mathbf{u}^h - \mathbf{u}_0^h)^T U''(\theta^h(\mathscr{T}))(\mathbf{u}^h - \mathbf{u}_0^h)\}_{ijk} \leq \sum_{i,j,k=0}^{N} h^3 \bar{U}(\mathbf{u}^{0,h}). \tag{2.9}$$

Observe that $U''(\theta^h(t))$, for $t \in [0, \mathscr{T}]$, is symmetric positive definite, since $\theta^h(t)$ is an intermediate state between $\mathbf{u}^h$ and $\mathbf{u}_0^h$. This implies that the thermodynamic variables of $\theta^h(t)$ are positive and bounded away from 0 since we have assumed that $\rho_{ijk} \geq 0$, $T_{ijk} \geq 0$. Hence, we obtain an L^2 bound on $\mathbf{u}^h$ (continuously in time). (This argument was given in [3] and also presented in [7].) The estimates on p^h and $(\rho(u^2+v^2+w^2))^h$ follows from the estimate of E^h and positivity. □

2.2 Positivity and solvability of the ODE system

The estimate in the previous section hinges on positivity, i.e., $\rho_{ijk}(t) \geq 0$ and $T_{ijk} \geq 0$. To demonstrate that the scheme produces positive solutions, we begin by considering positivity of ρ. The scheme for the continuity equation is:

$$(\rho_{ijk})_t + D_0^x(\rho u)_{ijk} + D_0^y(\rho v)_{ijk} + D_0^z(\rho w)_{ijk} = D_-^x\left(\frac{h\lambda^1_{i+1/2jk}}{2} D_+^x \rho_{ijk}\right)$$
$$+ D_-^y\left(\frac{h\lambda^2_{ij+1/2k}}{2} D_+^y \rho_{ijk}\right) + D_-^z\left(\frac{h\lambda^3_{ijk+1/2}}{2h} D_+^z \rho_{ijk}\right)$$

We present the argument for the terms in the x-direction keeping in mind that the other two directions are treated similarly. Hence, we consider,

$$(\rho_{ijk})_t + D_0^x(\rho u)_{ijk} + \cdots - D_-^x\left(\frac{h\lambda^1_{i+1/2jk}}{2} D_+^x \rho_{ijk}\right) - \cdots = 0$$

which can be restated as,

$$(\rho_{ijk})_t + \left(\frac{(u_{i+1} - \lambda^1_{i+1/2})\rho_{i+1} + (\lambda^1_{i+1/2} + \lambda^1_{i-1/2})\rho_i + (-u_{i-1} - \lambda^1_{i-1/2})\rho_{i-1}}{2h}\right)_{jk} \cdots = 0.$$

For any given $h > 0$, let ρ_i be the minimum. If $\rho_i \to 0$ then $(\rho_i)_t \geq 0$ since $\lambda^1_{i+1/2jk} \geq max(|u_{i+1jk}|, |u_{ijk}|)$. (The terms in the yz-directions are balanced by the same argument.) Hence, $\rho_i \geq 0$ and ρ^h will always remain non-negative. (The argument is based on the one given in [10].)

For positivity of p^h, we rely on Lax–Friedrichs scheme being entropy stable for any entropy. Then we can use the minimum entropy principle derived by Tadmor in [8]. From this result we have $S = \log(p\rho^{-\gamma}) \geq S_{min}$, at each point, or $p \geq \exp(S_{min})\rho^\gamma$, and positivity of p follows that of ρ. Finally, $T^h \geq 0$ follows from ρ^h, $p^h \geq 0$ and the gas law.

Next, consider a solution up to a time τ, where $\rho^h(t) \geq 0$ for all $t \in (0, \tau]$. Hence, Proposition 2.1 holds on this time interval. (Also, keep in mind that h is fixed for a particular approximation implying that the conservative variables are pointwise bounded from above thanks to the L^2 estimates.) Since $(\rho_{ijk})_t \geq 0$, we conclude that $(\rho_{ijk}) \geq 0$ in a neighborhood of $t = \tau$. Hence, we can extend our a priori bounds beyond $t = \tau$, and repeat the argument till we reach any finite time $\mathscr{T}$ (for all $h > 0$).

We summarize the results of this section.

Lemma 2.1 *Let the initial data satisfy Assumption 2.1. Then a semi-discrete solution of (2.2) satisfies $\rho_{ijk}(t), T_{ijk}(t) \geq 0$ for all $t \in [0, \mathscr{T}]$ and $i, j, k = 1 \ldots N$.*

The semi-discrete system constitutes a system of ordinary differential equations (ODEs), $\mathbf{u}^h_t = \mathscr{F}(\mathbf{u}^h)$, where $\mathscr{F}(\mathbf{u}^h)$ symbolizes the spatial discretization of (2.2). Having a priori determined the non-negativity of the numerical approximations, we turn to the question of solvability of the resulting ODE system.

We know that the a priori estimates can be extended to any finite time $\mathscr{T}$. From these estimates it is straightforward to show that for a given grid size h, the function $\mathscr{F}$ is Lipshitz continuous and hence there exists a unique solution on the arbitrary,

but finite, interval $[0, \mathscr{T}]$. *Consequently, we can generate a sequence of solutions* $\mathbf{u}^h$ *satisfying the a priori bounds given in Proposition* 2.1 *and Lemma* 2.1.

2.3 Estimates for strictly positive sequences

The estimates obtained from entropy considerations along with non-negativity are not enough to establish convergence to a weak solution. However, at this point we know that we can generate a sequence of solutions using the numerical scheme.

It is well-known that vacuum creates mathematical problems. Here, we can not preclude formation of vacuum regions in the limiting solution. However, close to vacuum (or generally large Knudsen numbers) the continuum hypothesis breaks down and the Euler equations are not valid. Hence, there is no practical limitation to henceforth consider sequences satisfying $\rho^h(t) \geq \epsilon > 0$. We will term this an *a posteriori condition* since we can examine its validity after a sequence has been generated.

Remark 2.2 Mathematically, one may argue that it is desirable to be able to prove that a weak solution is obtained even in the presence of vacuum. However, such a solution is not physically admissible. Consequently, it must be subject to the same a posteriori examination to ensure admissibility.

Lemma 2.2 *If* $\rho^h(t) \geq \epsilon > 0$, *uniformly as* $h \to 0$, *then* $T^h \in L^2(\Omega_N)$ *and* $\mathbf{v}^h \in (L^2(\Omega_N))^3$.

Proof By the gas law: $T^h \leq p^h/(R\epsilon) \in L^2(\Omega_N)$. From the L^2 estimates of the momentum components, we get the L^2 estimates on the velocities themselves. E.g. $u^h \leq \frac{(\rho u)^h}{\epsilon} \in L^2(\Omega_N)$. □

We can now bound the artificial diffusion terms in the numerical fluxes.

Lemma 2.3 *Under the assumptions of Proposition* 2.1 *and Lemma* 2.2, $h\lambda^{1,2,3} D_+^{x,y,z} u^k \in L^1(0, \mathscr{T}; L^1(\Omega_N))$, $k = 1 \ldots 5$.

Proof First, $\lambda^{1,2,3}$ depend on velocity and the speed of sound, i.e., $\sqrt{T}$, which are bounded by Lemma 2.2 in $L^\infty(0, \mathscr{T}; L^2(\Omega_N))$. Furthermore, hD_+u^k is bounded thanks to $\mathbf{u}^h \in C(0, \mathscr{T}; (L^2(\Omega_N))^5)$ by Proposition 2.1. The result follows by Cauchy–Schwarz. □

2.4 Equi-integrability of the numerical flux

The next step is to establish weak convergence in L^1 of the numerical fluxes.

Lemma 2.4 *Under the assumptions of Proposition* 2.1 *and Lemma* 2.2, *the numerical fluxes* $\mathbf{f}^{1,2,3}$ *are bounded in* $L^1(\mathscr{Q})$.

Proof The fluxes $\mathbf{f}^{1,2,3}$ are arithmetic averages of $\mathbf{g}^{1,2,3}$ plus artificial diffusion terms. Note that the entries of $\mathbf{g}^{1,2,3}$ are products of $\mathbf{u}^h$ or p^h, and $\mathbf{v}^h$. Consequently, the estimates of $\mathbf{g}^{1,2,3}$ follow from $\mathbf{u}^h \in L^2(\Omega_N)$, Lemma 2.2 and Cauchy-Schwarz. The artificial diffusion terms are bounded by Lemma 2.3. □

L^1 integrability is not sufficient for weak convergence. For that we need a slightly stronger bound, namely equi-integrability. There are a number of equivalent conditions for equi-integrability. We use the following:

Let $\mathscr{U} \in L^1(\mathscr{Q})$ be a family of integrable functions, then $\mathscr{U}$ is equi-integrable if and only if,

$$\lim_{\xi \uparrow \infty} \sup_{u \in \mathscr{U}} \int_{|u|>\xi} |u| \, dx = 0. \tag{2.10}$$

(For more information on equi-integrability, see [2]).

Lemma 2.5 *Under the assumptions of Proposition 2.1 and Lemma 2.2, the numerical fluxes* $\mathbf{f}^{1,2,3}$ *are equi-integrable.*

Proof Outline of the proof: We need to prove, term by term, that the numerical fluxes (2.3) are equi-integrable. From Lemma 2.4 the numerical fluxes are in L^1 and we only have to show that the fluxes satisfy (2.10), which is a condition on the local growth rate. We will use the artificial diffusion to bound the growth rate. Since it is a local condition, we consider the case where all the growth is concentrated in a single cell and show that this still leads to equi-integrability.

From the entropy estimate, and with our definition of λ, it is easy to see that we obtain an estimate of

$$\delta \int_0^{\mathscr{T}} \sum_{ijk=1}^{N} \left(h(D_+^x \mathbf{u}_{ijk}^h)^2 + h(D_+^y \mathbf{u}_{ijk}^h)^2 + h(D_+^z \mathbf{u}_{ijk}^h)^2 \right) h^3 \, dt \leq \mathscr{C}. \tag{2.11}$$

Hence, $D_+^{x,y,z}(\sqrt{h}\mathbf{u}^h) \in L^2(0, \mathscr{T}; L^2(\Omega_N))$. By Sobolev embedding, $\sqrt{h}\mathbf{u}^h \in L^2(0, \mathscr{T}; L^6(\Omega_N))$ (in three space dimensions). Furthermore, $\rho \geq \epsilon > 0$, gives $\sqrt{h}\mathbf{v}^h(L^2(0, \mathscr{T}; L^6(\Omega_N)))^3$.

Since for any fixed finite N the L^2 estimates imply bounds in $L^\infty(\Omega_N)$, we only need to investigate equi-integrability when $N \to \infty$. That is, $N \to \infty$ gives the supremum of the family $\mathscr{U} = \{\mathbf{u}^h\}$ in (2.10). (Or rather, if it does not give the supremum, $\{\mathbf{u}^h\}$ is equi-integrable since we would have a uniform bound in $L^\infty(\mathscr{Q})$.) Equi-integrability concerns the measure of max $|u|$. Hence, we consider the worst case scenario: all mass is concentrated on $h^3 \times \Delta t$ part of the domain $\mathscr{Q}$.

Remark 2.3 It is only if $\mathbf{u}^h$ is not in L^∞ that it might not be equi-integrable. Furthermore, the measure, $h^3 \times \Delta t$, of the set where mass is concentrated, can be replaced by any larger but vanishing set of width $H^3 \times \Delta \tilde{t}$. It has to be a vanishing set or else, the maximum will not grow out of bounds. However, the patch can not have a smaller width than h so that determines the maximal growth.

Consider the lth component of $\mathbf{u}^h$, here denoted u_{ijk}^l and let u^l be its maximum on the small patch of measure $h^3 \times \Delta t$. Given that, $\sqrt{h}\mathbf{u}^h \in L^2(0, \mathscr{T}; L^6(\Omega_N))$, we have

$$\int_0^T \sum_{ijk=1}^{N} ((\sqrt{h}u^l_{ijk})^6 h^3)^{2/6}\, dt \leq C.$$

Hence, if all mass is concentrated on the small subset.

$$\begin{aligned} ((\sqrt{h}u^l)^6 h^3)^{2/6} \Delta t &\leq C \\ ((u^l)^6 h^6)^{1/3} \Delta t &\leq C \\ (u^l)^2 h^2 \Delta t &\leq C \\ |u^l| &\leq C \frac{1}{\sqrt{\Delta t h}}. \end{aligned}$$

The velocities will also satisfy the analogous estimates. We now estimate a flux component, $\mathbf{g}$ proportional to $\mathbf{u}$ times a velocity component. (Here, we take the y-component v as a generic example.)

$$\begin{aligned} \lim_{\xi\uparrow\infty} \lim_{N\uparrow\infty} \int_{|\mathbf{g}|>\xi} |\mathbf{g}|\, d\mathbf{x}\, dt &\leq \lim_{\xi\uparrow\infty} \lim_{N\uparrow\infty} \int_{|\mathbf{g}|>\xi} |vu^l| d\mathbf{x}\, dt \\ &\leq \lim_{N\uparrow\infty} \left(C \frac{1}{\sqrt{\Delta t h}} \right)^2 h^3 \Delta t \sim \lim_{N\uparrow\infty} h = 0. \end{aligned} \tag{2.12}$$

There are also flux components proportional to "velocity times pressure". Hence, we need a maximal growth of pressure which can be obtained from the L^2 estimate of p^h. It is easy to see that on the same patch, we have

$$p_{max} \leq \frac{C}{\sqrt{\Delta t} h^{3/2}}. \tag{2.13}$$

Hence, with $\mathbf{g}$ now symbolizing, say vp, we have

$$\lim_{\xi\uparrow\infty} \lim_{N\uparrow\infty} \int_{|\mathbf{g}|>\xi} |vp_{max}| d\mathbf{x}\, dt \leq \lim_{N\uparrow\infty} C \frac{1}{\sqrt{\Delta t h}} \frac{1}{\sqrt{\Delta t} h^{3/2}} h^3 \Delta t \sim \lim_{N\uparrow\infty} \sqrt{h} = 0. \tag{2.14}$$

For the artificial diffusion term, we apply the same argument noting that one part is proportional to $\mathbf{v}^h \mathbf{u}^h$ and is bounded as in (2.12). The part involving the speed of sound is straightforward, since the sound speed ($\sim\sqrt{T}$) is bounded in $C(0, \mathscr{T}; L^4(\Omega_N))$. This term is approaching 0 somewhat faster than the term in (2.12). □

2.5 Convergence of flux terms

Equi-integrability ensures that a subsequence converges weakly in L^1. E.g., the momentum terms in the continuity equations $m^{1,h} \rightharpoonup m^1$. In this case, this immediately establishes that the continuity equation is satisfied weakly. However, for the

momentum and energy equations more information is needed. Consider the momentum equations. Equi-integrability gives

$$u^h m^{1,h} \rightharpoonup \overline{um^1} \in L^1,$$
$$p^h \rightharpoonup \overline{p^h} \in L^1.$$

(Similarly for all the other products of velocity and momentum). The pressure term needs no further attention but the momentum term does. We know that

$$u^h \rightharpoonup \overline{u} \in L^1, L^2, \quad m^{1,h} \rightharpoonup \overline{m^1} \in L^1, L^2,$$

and must show that $\overline{um^1} = \overline{u}\,\overline{m^1}$. Thanks to equi-integrability of the sequence $u^h m^{1,h}$, and weak convergence of u^h and $m^{1,h}$ it is sufficient to prove that either u^h or $m^{1,h}$ converges a.e. (sub-sequentially).

To prove this, we will, once again, use the artificial diffusion. However, we will need the following technical assumption.

Assumption 2.2 Assume that the sequence $\mathbf{u}^h$ of numerical solutions, satsify $\sqrt{h}(D_+^{x,y,x}\mathbf{u}^h_{ijk}) \in L^\infty(0, \mathscr{T}, L^2(\Omega_N))$.

Remark 2.4 This assumption rules out that the artifical diffusion term oscillates wildly in time. (Something that should be apparent in a simulation if it was not true.)

From (2.11) we have,

$$\int_0^{\mathscr{T}} \sum_{i,j,k=1}^{N} h^3 \frac{|\Delta m^{1,h}_{i+1/2,j,k}|^2}{h}\, dt < C. \tag{2.15}$$

First, we check how this estimate caps the formation of concentrations. Assume we localize all "mass" of the integrals to one point, say $\mathbf{x}_{mnp}$. Then

$$\int_0^{\mathscr{T}} |\Delta m^1_{m+1/2np}|^2\, dt < \frac{C}{h^2}. \tag{2.16}$$

In this special case, we conclude that the estimate ensures that $D_+^x m^{1,h} \in L^1(\Omega_N \times [0, \mathscr{T}])$. To see this we consider,

$$\int_0^T \|D_+^x m^{1,h}\|_1\, dt = \int_0^{\mathscr{T}} \sum_{i,j,k=1}^{N} h^3 \frac{|\Delta m^1_{i+1/2jk}|}{h}\, dt < C$$

which, with all mass located at one point,

$$\int_0^{\mathscr{T}} |\Delta m_{m+1/2np}|\, dt < \frac{C}{h^2}. \tag{2.17}$$

With $|\Delta m^1_{m+1/2np}| > 1$, (2.16) dominates (2.17). A similar argument reveals that (2.15) bounds $\|D^x_+ m^{1,h}\|_1$ on sets up to $\mathscr{O}(N^2)$ points. Hence, concentrations will not destroy the a.e. convergence, since if $m^{1,h} \in L^1(0, \mathscr{T}; W^{1,1}(\Omega_N))$ and by Assumption 2.2, we would have strong convergence of a subsequence in $L^1(0, \mathscr{T}; L^{3/2}(\Omega_N))$.

Remark 2.5 We stress that we have not proven that $m^{1,h} \in L^1(0, \mathscr{T}; W^{1,1}(\Omega_N))$ in general. We only claim that families of functions with mass concentrated on sets less than $\mathscr{O}(N^2)$, are bounded in $L^1(0, \mathscr{T}; L^{3/2}(\Omega_N))$. Consequently, we can draw from such an (infinite) family of functions a strongly convergent subsequence in $L^{3/2}$.

What is left to prove is that oscillations are kept at bay such that a.e. convergence can be inferred. Hence, we consider an $\mathscr{O}(N^3)$ set, denoted $\mathscr{B}_{N^3}$. (The general case $\mathscr{O}(N^2 N^\alpha)$, $\alpha \in (0, 1]$, is straightforward to handle in a similar way.)

On such a set, we obtain from (2.15) that every difference is bounded as

$$\int_0^{\mathscr{T}} |\Delta m^1_{m+1/2np}|^2 \, dt < Ch, \quad \text{for all} \quad (x_m, y_n, z_p) \in \mathscr{B}_{N^3}. \tag{2.18}$$

Unfortunately, this will not bound $\|D^x_+ m^{1,h}\|$ but it clearly shows that the differences are decreasing to 0. The highest frequency in the x-direction is proportional to $a_N \sin(Nx)$. Hence, $a_N(\sin(Nx) - \sin(N(x+h))) \sim a_N Nh \sim a_N$, where h is the grid step. We conclude that $a_N \sim \sqrt{h}$. Hence, we obtain a.e. convergence of $m^{1,h}$ for such functions. *By this we have shown that $m^{1,h}$ converges a.e. on any subset of Ω_N. In conjunction with equi-integrability, we conclude that $\overline{um^1} = \overline{u}\,\overline{m^1}$.* (Assumption 2.2 ensures that oscillations in time do not destroy convergence.)

Moving to the energy equation, we can make the same argument to prove convergence of $u^h E^h$-type terms. To prove that $u^h p^h$ converges, we observe that this follows from weak convergence of $m^{1,h} T^h \in L^1$, $m^{1,h} \rightharpoonup m^1 \in L^1$ and *almost everywhere*, and weak convergence of $T^h \in L^2$.

Finally, we need to show that the artificial diffusion terms converge to 0 weakly in L^1. We denote the artificial diffusion part of $\mathbf{f}^1_{i+1/2jk}$ in (2.3) as

$$\mathbf{g}^{AD,1}_{i+1/2jk} = \frac{h\lambda^1}{2} D^x_+ \mathbf{u}^h_{ijk}. \tag{2.19}$$

(Similarly for the other two fluxes.) We first note that thanks to the a priori estimates, we have

$$\sqrt{h\lambda^1} D^x_+ \mathbf{u}^h_{ijk} \in L^2(0, \mathscr{T}, L^2(\Omega_N)). \tag{2.20}$$

As already noted, $\lambda^1 (\sim |u| + \sqrt{T}) \in L^2(0, \mathscr{T}, L^2(\Omega_N))$. By Cauchy-Schwarz,

$$\mathbf{g}^{*,1}_{i+1/2jk} = \frac{\mathbf{g}^{AD,1}_{i+1/2jk}}{\sqrt{h}} = \frac{\sqrt{h}\lambda^1}{2} D^x_+ \mathbf{u}^h_{ijk} \in L^1(\mathscr{Q}).$$

From (2.12), the artificial diffusion flux satisfies the equi-integrability relation

$$\lim_{\xi\uparrow\infty}\lim_{N\uparrow\infty}\int_{|\mathbf{g}^{AD,1}|>\xi}|\mathbf{g}^{AD,1}|\,d\mathbf{x}\,dt\sim\lim_{N\uparrow\infty}h=0. \tag{2.21}$$

and, therefore, the function $\mathbf{g}^{*,1}=\frac{\mathbf{g}^{AD,1}}{\sqrt{h}}$, is also equi-integrable, and we can extract a convergent subsequence that converges weakly in $L^1(\mathscr{Q})$. We conclude that $\mathbf{g}^{AD,1}=\sqrt{h}\mathbf{g}^{*,1}$ converges weakly in L^1 to 0.

We summarize the results in a proposition.

Proposition 2.2 *Let* $\mathbf{u}^h$, *on* $\mathscr{Q}=\Omega_N\times[0,\mathscr{T}]$ *be a sequence of solutions generated by the scheme* (2.2) *with* $\rho_{ijk}(t)\geq\epsilon>0$ *and satisfying Assumption* 2.2. *Then for a subsequence, the numerical fluxes* (2.3) *converge weakly in* $L^1(\mathscr{Q})$.

2.6 Entropy solutions

At this point, we can summarize our findings in the main theorem.

Theorem 2.3 *The scheme* (2.2) *generates a sequence of numerical solutions*, $\mathbf{u}^h$, *on* $\Omega_N\times[0,\mathscr{T}]$. *If the sequence satisfies* $\rho_{ijk}(t)\geq\epsilon>0$ *and Assumption* 2.2, *then a subsequence converges weakly to an entropy solution of the Euler equations* (1.1).

Proof First, the scheme satisfies the entropy stability condition (2.7), which ensures that a weak solution is also an entropy solution.

Multiplying (2.2) by test functions $\phi\in\mathscr{D}(\mathscr{Q})$ (projected onto the grid) it is straightforward to move the spatial differences onto the test function using summation by parts and periodicity.

$$\int_0^T\sum_{ijk=1}^N h^3\Big((\phi_{ijk})_t\mathbf{u}_{ijk}+(D_+^x\phi_{ijk})\mathbf{f}^1_{i+1/2jk}+(D_+^y\phi_{ijk})\mathbf{f}^2_{ij+1/2k}+(D_+^z\phi_{ijk})\mathbf{f}^3_{ijk+1/2}\Big)\,dt$$
$$+h^3\sum_{ijk=1}^N\phi_{ijk}(0)\mathbf{u}^{h,0}_{ijk}=0. \tag{2.22}$$

Equation (2.22) will converge to (1.3) in a distributional sense, if $\mathbf{u}^h,\mathbf{f}^m_{ijk}$ are (at least) equi-integrable and the fluxes $\mathbf{f}^i(\mathbf{u}^h)\rightharpoonup\mathbf{f}^i(\mathbf{u})$. By Proposition 2.1 $\mathbf{u}^h\in C(0,\mathscr{T};L^2(\Omega_N))$ and a subsequence will converge weakly. The fluxes are equi-integrable by Lemma 2.5 and a subsequence converges in $L^1(\mathscr{Q})$. Finally, by Proposition 2.2, we have $\mathbf{f}^i(\mathbf{u}^h)\rightharpoonup\mathbf{f}^i(\mathbf{u})$ and we conclude that the limit is a weak solution. □

We make a few remarks on the implications of this theorem.

- Equation (1.1) is satisfied in $\mathscr{D}'(\mathscr{Q})$ but $\mathbf{u}^h$ will converge weakly in L^2 (and L^1).
- In smooth regions, i.e, where the solution is differentiable, the effect of the artificial diffusion will vanish as $h\to0$.

– While the thermodynamic variables remain positive till any finite time, the scheme can not preclude the appearance of large vacuum regions. Nevertheless, the numerical solution, $\mathbf{u}^h$, will remain bounded but the velocities and temperature may not be bounded. Under such circumstances, $\{\mathbf{u}^h\}$ *may* not approximate a weak solution.
– It is possible to relax the scheme to the standard local Lax–Friedrichs by setting $\delta = 0$. We only need to use (2.11) for sequences with $\rho, T \geq constant > 0$, since it is only for such sequences we are able to prove convergence to weak solutions. Moreover, for such sequences, we have an estimate (2.11) with $\sqrt{T_{min}}$ in place of δ. (The minimum of the speed of sound.)

We also note that Lax–Friedrichs scheme is not the only scheme satisfying estimates like the ones derived above (excluding positivity). All entropy stable schemes do. (See [9] for a definition of entropy stability.) These include entropy-fixed Roe, Godunov and others. There are also several examples of high-order entropy stable schemes, which have wider stencils and are usually less diffusive. It is a non-trivial task to prove that the estimates at hand are sufficient for convergence of more complicated numerical fluxes. In general, convergence can not be assumed based on the estimates alone.

3 Kelvin–Helmholtz problem

As an example of entropy solutions obtained with Lax–Friedrichs scheme, we consider a Kelvin–Helmholtz problem. (Here, we use $\delta = 0$.) This problem was proposed in [4] as a sensitive test case for the Euler equations, and we have used the same set-up. The initial conditions are given by

$$\mathbf{u}^0 = \begin{cases} \mathbf{u}_1 & \text{if } 0.25 < y < 0.75 \\ \mathbf{u}_2 & \text{if } y \leq 0.25 \text{ or } y \geq 0.75 \end{cases} \tag{3.1}$$

where $\mathbf{u}_1$ and $\mathbf{u}_2$ are the conservative variables obtained from the states: $\rho_1 = 2$ and $\rho_2 = 1$; $u_1 = -0.5 + \epsilon \sin(2\pi x)$ and $u_2 = 0.5 + \epsilon \sin(2\pi x)$; $v_1 = v_2 = 0 + \epsilon \sin(2\pi y)$; $p_1 = p_2 = 2.5$. With $\epsilon = 0$, $\mathbf{u}^0$ is a steady state solution of the Euler equations. To trip the instability and obtain a time dependent solution we set $\epsilon = 0.1$. This will produce the familiar Kelvin–Helmholtz swirls. In the presence of shear stress (i.e. with the Navier-Stokes equations), these swirls usually break up in smaller vortices and the flow may even become turbulent. Without any shear stress (the Euler equations), the swirls roll up as vortex sheets.

The results from running Lax–Friedrichs scheme (with Euler-forward in time) till $\mathscr{T} = 2$ are shown in Table 1. We present the L^1 norms of ρu and ρv. The L^2-norm values are given for ρ and E since the L^1 norms are constant (too machine precision) thanks to positivity and conservation. Furthermore, we tabulate the L^1-differences of the variables on consecutive grids. Upon convergence, these values should approach 0.

As seen in Table 1, the L^1-/L^2-norms of the variables are converging. The differences are also decreasing and form Cauchy sequences. The only deviance is in ρv where there is a large decrease between 2048^2 and 4096^2 followed by a slight increase (8192^2) and a substantial decrease to the finest grid (16384^2). It is not unexpected

Table 1 L^2/L^1-norm values of variables and L^1-differences between two consecutive refinements

N	ρ		E		ρu		ρv	
	L^2	L^1-diff	L^2	L^1-diff	L^1	L^1-diff	L^1	L^1-diff
512	1.5557	–	6.4488	–				
1024	1.5637	0.076	6.4521	0.13	0.5651	–	0.09254	–
2048	1.5706	0.070	6.4573	0.10	0.5818	0.067	0.1329	0.058
4096	1.5756	0.052	6.4602	0.052	0.5886	0.036	0.1790	0.021
8192	1.5802	0.040	6.4629	0.051	0.5959	0.023	0.1858	0.024
16384	1.5842	0.038	6.4653	0.045	0.6034	0.022	0.1876	0.016

that the sequence is not perfectly decreasing since there is dynamics in between the variables. Nevertheless, it should be clear that the simulations indicate convergence.

In Fig. 1, the solutions on the sequence of grids are shown. Finer structures appear on finer grids and the large structures become better resolved. We also see the roll-up of the vortex sheets.

Remark 3.1 For smooth solutions, the convergence of Lax–Friedrichs should be 1 (based on linear theory). In Table 1, the convergence is less than 1, but the solution is non-smooth. The theory in this paper does not predict convergence rates, which could be very slow. However, if the convergence were to stall on a finer grid, at least one of the two assumptions must have failed. That is, the solution would have to start to develop a vacuum not noticed on the existing grids, or begin to oscillate wildly in time.

Next, we investigate the behaviour as $\epsilon \to 0$. We compute numerical solutions $\mathbf{u}_\epsilon^h$ till $\mathscr{T} = 2$ for a decreasing sequence of ϵ values. With $\epsilon = 0$, we should expect to see $\mathbf{u}^0$ unchanged in time since it is a steady state solution. In Table 2 the L^1 and L^2 differences between $\mathbf{u}_\epsilon^h$ and $\mathbf{u}^0$ are listed.

The first part of Table 2 shows the sequence of errors as ϵ decreases, computed on a grid with $N^2 = 1024^2$ grid points. We note that the errors decrease towards 0, as they should, but they do not reach 0 when $\epsilon = 0$. The reason is that the artificial viscosity diffuses the discontinuity and introduces an error proportional to the grid size. Hence, we should see a further reduction of the error if the resolution is increased. Indeed, that is the case. The discontinuity becomes sharper, as depicted in Fig. 2, and we see in the last two rows of Table 2 that the error continues to decrease towards zero.

Our numerical results for the Kelvin–Helmholtz problem contradict those presented in [4], where numerical solutions were generated by an entropy-stable high-order ENO scheme (termed TeCNO). Their solutions were "turbulent-like" in that smaller and smaller, seemingly random, vortices were introduced on finer grids. Similarly, they report that there is no convergence to the steady state solution when the initial perturbation vanish.

In this regard, we remark that the Kelvin–Helmholtz roll-ups generated by the standard Lax–Friedrichs scheme are well-known and observed both in nature and experiments. Furthermore, it seems reasonable that in the ideal case of no physical viscosity, and no initial perturbation, the Kelvin–Helmholtz instability would not be

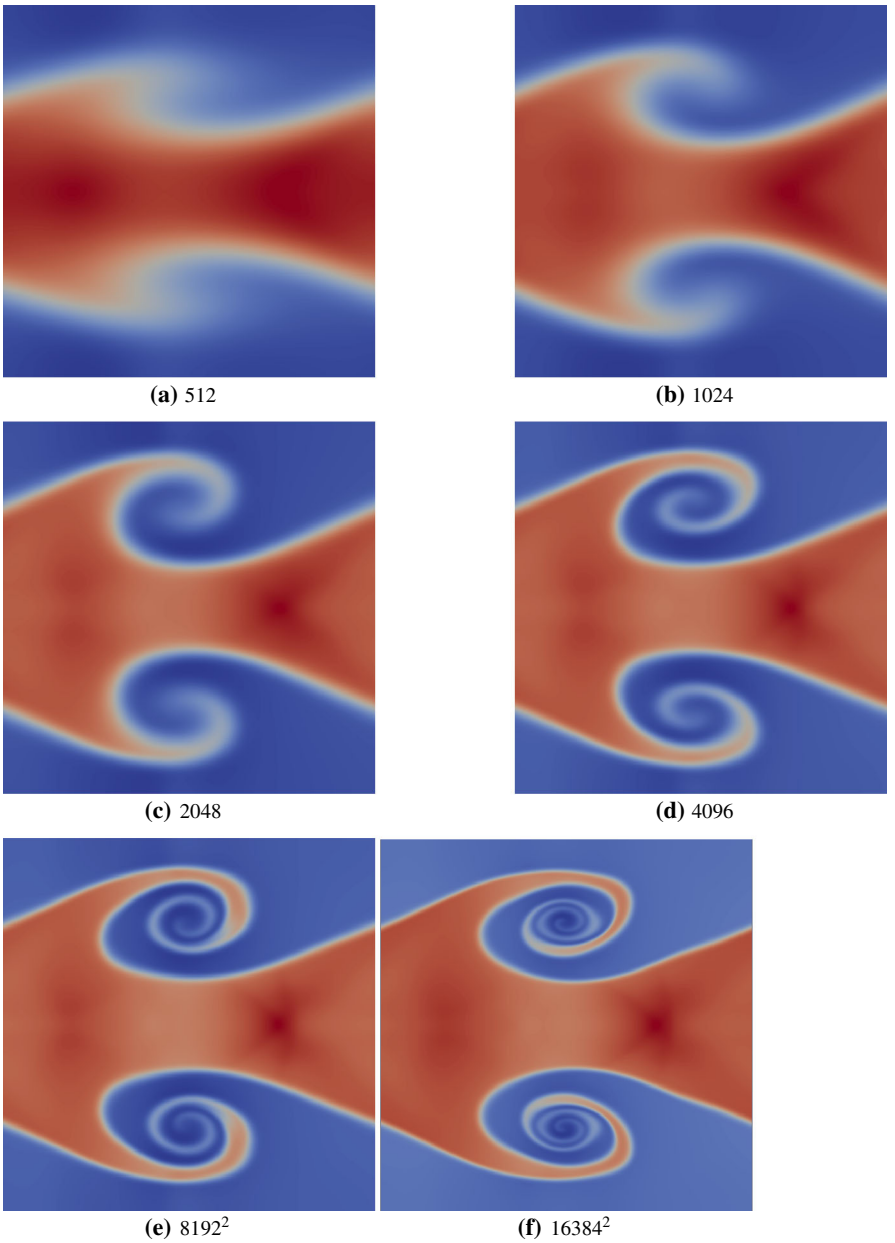

(a) 512 **(b)** 1024

(c) 2048 **(d)** 4096

(e) 8192^2 **(f)** 16384^2

Fig. 1 Figures of density at $\mathscr{T} = 2.0$ on different grids. $\epsilon = 0.1$

tripped. (The sheets of fluid would simply slip by each other as is the case in the Lax–Friedrichs solution.)

A few properties of the Lax–Friedrichs scheme are: it is locally diffusive; the stencil does not change between points; the scheme is everywhere linearly stable. As a sim-

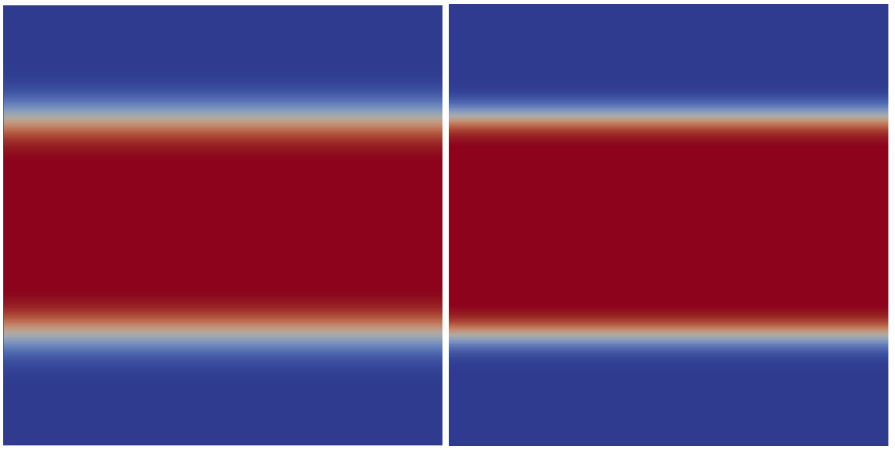

(a) 2048^2 **(b)** 4096^2

Fig. 2 Figures of density at $\mathscr{T} = 2.0$ on different grids with $\epsilon = 0$

Table 2 ϵ-convergence measured in ρ. Difference between steady state solution and numerical solution at $\mathscr{T} = 2$

N	ϵ	L^1	L^2
1024	0.1	0.205	0.344
1024	0.01	0.0922	0.166
1024	0.0	0.0898	0.160
2048	0.0	0.0644	0.135
4096	0.0	0.0431	0.1039

ple test of the influence of the diffusive terms, the Kelvin–Helmholtz problem (with perturbation) was run with the same code but with a smaller diffusion coefficient. All simulations remained stable and positive but when the diffusion was about an order of magnitude less than the standard Lax–Friedrichs, roll-ups on smaller scales grows, creating a "turbulent-like" behavior. Hence, it appears that the level of diffusion determines whether or not unresolved numerical noise is damped or if the Kelvin–Helmholtz instability is allowed to amplify the perturbation.

4 Conclusions

We have shown that in the regime where the Euler equations constitute a valid physical model, there exists (weak) entropy solutions for possibly large but appropriately bounded initial data. This was accomplished by using the standard local Lax–Friedrichs scheme, which has the following key features:

– It *always* produces a numerical solution to any finite time $\mathscr{T}$.
– If, and this condition can be examined *a posteriori*, the density remains bounded away from 0, the scheme is *convergent* to a weak solution.

– The scheme is entropy stable for all entropies and the approximated weak solution is an *entropy solution*.

We have already stressed the importance of the second point but emphasize it again. We do not use positivity as an a priori assumption. It is only used to determine whether or not a weak solution has been recovered. If vacuum occurs, we do not get a weak solution but even *IF* a weak solution exists, it would not model physics since the Euler equations do not constitute a valid model for vacuum. So from a modeling perspective, this a posteriori examination should anyway be carried out.

In Sect. 3, we presented numerical results for a Kelvin–Helmholtz problem, obtained with the Lax–Friedrichs scheme. We observed strong convergence in L^1. Furthermore, we demonstrated that the steady state solution is recovered when the perturbation $\epsilon \to 0$ and the grid is refined. In summary, the numerical experiments corroborate the theoretical findings.

Acknowledgements The author wishes to thank Prof. Henrik Kalisch for valuable discussions.

References

1. Bianchini, S., Bressan, A.: Vanishing viscosity solutions of non-linear hyperbolic systems. Ann. Math. **161**, 223–342 (2005)
2. Brezis, H.: Functional Analysis, Sobolev Spaces and Partial Differential Equations. Springer, New York (2010)
3. Dafermos, C.M.: Hyperbolic Conservation Laws in Continuum Physics. Springer Verlag, Berlin (2000)
4. Fjordholm, U.S., Käppeli, R., Mishra, S., Tadmor, E.: Construction of approximate measure valued solutions for hyperbolic systems of conservation laws. Technical Report. Cornell University Library (2014). To appear in Foundations of Computational Mathematics. arXiv:1402.0909
5. Harten, A.: On the symmetric form of systems of conservation laws with entropy. J. Comput. Phys. **49**, 151–164 (1983)
6. Slemrod, M.: Admissibility of weak solutions for the compressible Euler equations, $n \geq 2$. Philos. Trans. R. Soc. A **371**, 1–11 (2013)
7. Svärd, M.: Weak solutions and convergent numerical schemes of modified compressible Navier-Stokes equations. J. Comput. Phys. **288**, 19–51 (2015)
8. Tadmor, E.: A minimum entropy principle in the gas dynamics equations. Appl. Numer. Math. **2**, 211–219 (1986)
9. Tadmor, E.: Entropy stability theory for difference approximations of nonlinear conservation laws and related time-dependent problems. Acta Numer. **12**, 451–512 (2003)
10. Tang, H.Z., Xu, K.: Positivity-preserving analysis of explicit and implicit Lax Friedrichs schemes for compressible Euler equations. J. Sci. Comput. **15**(1), 19–28 (2000)